

Trapping of surface-plasmon polaritons in a graded Bragg structure: Frequency-dependent spatially separated localization of the visible spectrum modes

Lin Chen,¹ Guo Ping Wang,^{1,*} Qiaoqiang Gan,² and Filbert J. Bartoli²

¹Key Laboratory of Acoustic and Photonic Materials and Devices, Ministry of Education and Department of Physics, Wuhan University, Wuhan 430072, China

²Center for Optical Technologies, Electrical and Computer Engineering Department, Lehigh University, Bethlehem, Pennsylvania 18015, USA

(Received 14 September 2009; published 30 October 2009)

We theoretically demonstrate that a metallic film covered by a dielectric grating of graded thickness can strongly slow light as the propagation velocities of surface plasmon polaritons (SPPs) are reduced over a large frequency bandwidth at visible frequencies. Since the dispersive relation of SPPs is dependent on the dielectric grating thickness, the guided SPPs at different frequencies can be localized at different spatial positions of the plasmonic grating. We numerically demonstrate that a true rainbow from violet to red colors can be separately localized, resulting in the spatial separation of the visible spectrum on a chip.

DOI: 10.1103/PhysRevB.80.161106

PACS number(s): 73.20.Mf, 42.25.Bs, 42.79.Gn, 78.68.+m

Slow light has attracted tremendous research interest because of a broad range of potential applications, including optical buffers,¹ filters,² and enhanced light-matter interactions.³ To address the needs of various applications, it is highly important to design novel structures and explore new mechanisms that can significantly slow down or even stop light.⁴ In recent years, a series of discoveries revealed that it is possible to obtain ultraslow light.^{5–8} Typical examples include the use of quantum interference effects,⁵ photonic crystals (PCs),⁶ stimulated Brillouin scattering,⁷ and electromagnetically induced transparency⁸ to achieve such a purpose.

As electromagnetic waves bounded to the interface of metals and dielectrics, surface plasmon polaritons (SPPs) offer a great potential for carrying optical signals in nanoscale networks.⁹ Currently, much effort is being focused on slowing light in plasmonic structures, i.e., the reducing group velocity (v_g) of SPPs.^{10,11} The concept of a “trapped rainbow” storage of terahertz light in metamaterial waveguides¹² and metal grating structures¹³ has attracted special attention because of the ability to stop light of different wavelengths at different positions. More recently, the metal grating structures have been successfully scaled to nanoscale level for a trapped rainbow in the telecommunication domain, or even in the visible domain.¹⁴ Alternatively, chirped photonic crystal waveguides or tapered plasmonic waveguides have been demonstrated to be capable of gradually slowing down and even stopping light waves.^{15,16} In this Rapid Communication, we demonstrate that a metal film covered by a dielectric grating with a graded thickness can trap a true rainbow, ranging from violet to red spectral regions. As a white light beam is coupled into the structure, each frequency component of the beam could be localized at different spatial positions, resulting in spatial separation of different colors in the visible spectrum, and lead to a real trapped rainbow at the nanoscale domain on a chip.

We first consider two plasmonic structures shown in insets A and B of Fig. 1. The dispersive relation of TM-polarized light modes (here, the SPP modes propagate along the z direction) in the metal-dielectric-air model (inset A of Fig. 1) can be expressed as

$$k_d h = \arctan\left(\frac{\epsilon_d k_a}{\epsilon_0 k_d}\right) + \arctan\left(\frac{\epsilon_d k_m}{\epsilon_m k_d}\right), \quad (1)$$

with $k_m = \sqrt{\beta^2 - \epsilon_m k_0^2}$, $k_d = \sqrt{\epsilon_d k_0^2 - \beta^2}$, $k_a = \sqrt{\beta^2 - \epsilon_0 k_0^2}$, and $n_{eff} = \beta/k_0$, where β is the propagation constant of TM modes in the dielectric layer and $k_0 (=2\pi/\lambda)$ represents the wave vector of light in the air. ϵ_m , ϵ_d , and ϵ_0 are the dielectric constants of metal, dielectric layer, and air, respectively. n_{eff} ($=n'_{eff} + jn''_{eff}$) is the effective refractive index of the SPP mode and h is the thickness of the dielectric layer. Figure 1 shows the dependence of n'_{eff} on the wavelength λ as a function of h . In the calculation, the dielectric layer is Si_3N_4 ($n_d = \sqrt{\epsilon_d} = 2.03$) while the metal film is silver, whose dielectric properties are described by the Drude model $\epsilon_m = 1 - f_p^2 / (f^2 + i\Gamma f)$ with the plasma frequency f_p , loss component Γ , and frequency of the incident light f , respectively. By fitting the experimental data¹⁷ as shown in inset (i) of Fig. 1 (n is the refractive index and k is the extinction coefficient),

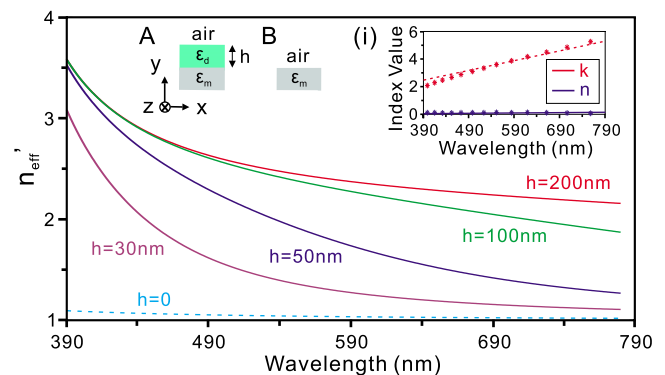


FIG. 1. (Color online) Dependence of the real part n'_{eff} of effective refractive index of SPPs on wavelength λ for different grating thicknesses h . Inset A: metal-dielectric-air model ($h \neq 0$, silver- Si_3N_4 -Air). Inset B: metal-air model ($h=0$, silver-air). Inset (i): optical properties of silver in the visible domain. Blue solid line: the refractive index n , and red dashed line: the extinction coefficient k .

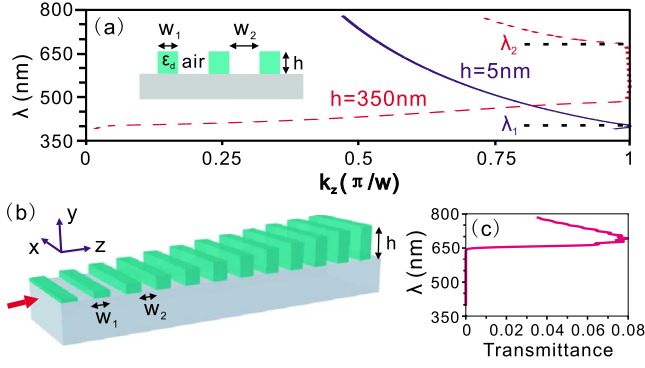


FIG. 2. (Color online) (a) Calculated band dispersion of a metallic film coated with a binary dielectric grating with thickness $h = 5$ nm (blue solid line) and 350 nm (red dashed line), respectively. The widths of the dielectric and air layers are set at $w_1 = 70$ nm and $w_2 = 110$ nm, respectively. Inset: schematic of the structure. (b) Schematic of the designed graded plasmonic structure (infinite along the x axis) for trapping rainbow in the visible domain. (c) Calculated transmittance of SPPs passing through the structure of (b). In the calculations, the grating thickness h increases linearly from 5 to 350 nm with the step of 2.5 nm, and the total length of the structure is approximately 25 μm . Other parameters are the same as that of (a).

we obtain $f_p = 2.04 \times 10^{15}$ Hz and $\Gamma = 9.37 \times 10^{12}$ Hz in the range of wavelength from 390 to 780 nm. From Fig. 1, one can see that n'_{eff} decreases with λ for a fixed h but increases with h for a given λ . This is consistent with previously reported results:¹⁸ the real part of the SPP wave vector increases monotonically with dielectric thickness if the frequency of the incident light is lower than the characteristic frequency of the metal-dielectric models. As the thickness of the dielectric layer decreases to $h=0$, which corresponds to the metal-air model (inset B of Fig. 1), the dispersion equation of SPPs becomes $\beta = 2\pi/\lambda \sqrt{\epsilon_0 \epsilon_m / (\epsilon_0 + \epsilon_m)}$. The corresponding SPP n'_{eff} values are also shown in Fig. 1 ($h=0$, cyan dashed line). From this figure we can see that n'_{eff} of SPPs in the metal-air model ($h=0$) is lower than that in the metal-dielectric-air model ($h \neq 0$) for a fixed λ in the visible domain. Therefore, similar to metal Bragg grating structures used to guide slow SPPs,¹¹ we can design a plasmonic Bragg waveguide by alternately stacking the two plasmonic models discussed above, which can be realized by coating a metallic film with a binary dielectric grating [see the inset of Fig. 2(a)], to guide slow SPP modes. The band dispersion of this periodic structure can be obtained from the well-known secular equation¹⁹

$$\cos kd = \cos k_1 w_1 \cos k_2 w_2 - \frac{1}{2} \left(\frac{n_1}{n_2} + \frac{n_2}{n_1} \right) \sin(k_1 w_1) \sin(k_2 w_2), \quad (2)$$

where k is the Bloch vector along the z axis, $d = w_1 + w_2$ is the lattice constant (w_1 and w_2 are the widths of the dielectric and air layers, respectively), and n_j and $k_j = n_j \omega / c$ ($j=1, 2$) are the effective refractive index and wave vector of SPPs in the metal-dielectric-air model ($j=1$) and metal-air model ($j=2$), respectively. From Eq. (2) we can obtain the SPP propa-

gation band structure in the plasmonic waveguide. Since n_1 is related to h in Eq. (1), the band dispersion will differ for different h . Our calculations reveal a redshift of the wavelength near the upper edge of the band gap with the increased thickness of the dielectric layer h , which is attributed to the fact that n_1 increases with h for a given λ (see Fig. 1). Figure 2(a) shows the calculated band dispersion of the structure with $h=5$ nm (blue solid line) and $h=350$ nm (red dashed line), respectively, where the widths of the dielectric layers and the air are fixed at $w_1 = 70$ nm and $w_2 = 110$ nm, respectively. It can be seen that, at $h=5$ nm, the wavelength λ at the upper edge of the gap is $\lambda_1 = 405$ nm while, at $h=350$ nm, λ shifts to $\lambda_2 = 680$ nm.

Following the fact that Bragg grating structure can strongly reduce v_g of the light near the edge of the band gap,¹¹ we can deduce that v_g of an SPP mode will be reduced as the incident light at $\lambda = \lambda_1 = 405$ nm (or $\lambda = \lambda_2 = 680$ nm) is coupled into the plasmonic structure with $h=5$ nm ($h=350$ nm). However, similar to PCs, such structures with a constant dielectric thickness h can only slow down SPPs within a very narrow frequency range near the edge of the band gap. Therefore, we design a planar plasmonic structure constructed by a metal film coated with a graded binary dielectric grating (infinite along the x axis) as shown in Fig. 2(b) to enlarge the bandwidth of the slow SPP modes. The coated grating thickness h is linearly increased from the left-hand side ($h=5$ nm) to the right-hand side ($h=350$ nm) along the z direction. Note from Fig. 2(a) that the wavelength λ of the upper edge of the band gap shifts from $\lambda_1 = 405$ nm to $\lambda_2 = 680$ nm as the grating thickness changes from $h=5$ to 350 nm. We conclude that the graded plasmonic structure shown in Fig. 2(b) can in principle slow down or confine the SPPs ranging from $\lambda_1 = 405$ nm to $\lambda_2 = 680$ nm. Figure 2(c) shows the calculated transmission spectrum of the designed plasmonic structure [Fig. 2(b)] in the visible domain from 390 to 780 nm, obtained by two-dimensional (2D) finite-difference time-domain (FDTD) simulations.²⁰ Considering the metallic dispersion and intrinsic loss, the iterative equation of 2D FDTD was modified according to the polarization equation approach.²¹ The total length of the structure is approximately 25 μm (140 periods). We can see that there exists a plasmonic band gap in the range of wavelength from 390 to 650 nm [see Fig. 2(c)], implying that SPPs in the band gap cannot pass through the structure but are localized at different spatial positions instead.

To confirm the prediction above, we employ the 2D FDTD method to simulate the magnetic field intensity distributions ($|H_x|^2$, where H_x is the magnetic field along the x axis) as SPPs pass through the plasmonic structure constructed by a metal Ag and a dielectric Si_3N_4 (Fig. 3). The excitation wavelengths are set at 390 (violet), 490 (blue), 560 (green), 585 (yellow), 610 (orange), and 635 nm (red), respectively, while all the other parameters are the same as that used in Fig. 2(c). From Fig. 3 we can see that SPPs excited by different wavelengths are localized at different spatial positions along the metal surface: the SPP modes excited by shorter wavelengths will be localized at the positions closer to the input port of the structure (with thinner h), while those launched by longer wavelengths will be localized at the positions further away from the input side of the structure (with

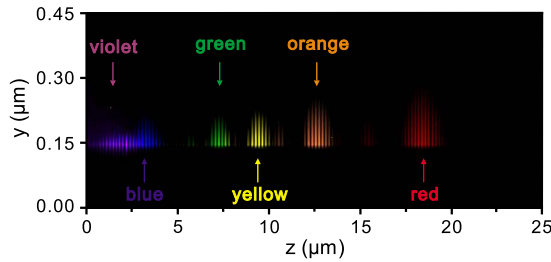


FIG. 3. (Color online) FDTD simulated magnetic field intensity distributions ($|H_x|^2$) of SPPs through the graded plasmonic structure shown in Fig. 2(b) as the incident light is at 390 (violet), 490 (blue), 560 (green), 585 (yellow), 610 (orange), 635 nm (red), respectively. Other parameters are the same as that of Fig. 2(c).

thicker h). Since the guided SPPs are localized at different spatial positions, we can conclude that v_g 's of SPPs are significantly reduced.

It was experimentally demonstrated that v_g of SPPs can be estimated by the time evolution of SPP pulse through the slow plasmonic waveguide structures.¹¹ Here, we will estimate v_g of SPPs using this method through FDTD simulation. In the calculations, a time-domain TM-polarized Gaussian pulse [magnetic field is parallel to the x axis; see Fig. 2(b)] with a pulse width (σ) of 90 fs, centered at a single wavelength is used. Figure 4(a) shows the calculated gray distribution of the SPP field intensity ($|H_x|^2$) in time-position plane (along the z axis, 5 nm above the metal surface) as a light pulse centered at 635 nm [within the band gap of the plasmonic structure; see Fig. 2(c)] is coupled into the structure. It can be seen that the field intensity of SPPs increases with both the propagation distance and time, and finally reaches its maximum, implying the localization effect or, in other words, the significant reduction in v_g .¹⁵ The short-range oscillation behavior along the propagation direction can be attributed to both the Bloch wave characteristics of the

guided SPPs and the interference between the forward and reflected SPPs.¹⁵

To more clearly show the time evolution of the SPP propagation, we present in Fig. 4(b) the dependence of the intensity profile of the SPPs on the propagation time at eight spatial positions of the structure, with a spacing of 2.5 μm along the propagation direction (the first position is 1.5 μm away from the input port of the structure). The figure shows that the SPPs around the last position (19 μm away from the input port) show the strongest intensity (red solid line), corresponding to the localization around the coordinate point (19 μm , 0.37 ps) of Fig. 4(a). On the other hand, Fig. 4(b) shows the propagation evolution of the SPP pulse along the plasmonic structure: the SPP wave packet arrives sequentially at the eight positions from the nearest one (1.5 μm away from the input port of the structure) to the furthest one (19 μm away from the input port) with a slower and slower group velocity. For example, it takes only about 10 fs for the SPP mode to pass through the first 2.5- μm -long distance (from 1.5 to 4 μm away from the incident port of the structure), while it takes about 80 fs for the last 2.5- μm -long distance (from 16.5 to 19 μm). The relation between the propagation distance and the propagation time of the SPP wave packet is plotted in the inset of Fig. 4(a). The curve becomes steeper and steeper with the increased propagation distance, clearly confirming the gradual slowing down of the SPP modes through the structure. Therefore, as incident light is coupled into the structure, v_g of the SPPs will gradually be slowed down and, in principle, eventually approach the “stopped” condition as the light frequency approaches the band-gap edge of the structure.

From the practical point of view, however, the SPPs can never be completely stopped due to the metallic absorption.²² For instance, v_g ($\equiv d\omega/dk$) of SPPs excited by the incident light ($\lambda=680$ nm) around the upper edge of the band gap of a plasmonic structure with a thickness of 350 nm [red dashed line in Fig. 2(a)] is approximately $c/15$ in our case. To suppress the effect of the metallic absorption, we can employ a gain medium to compensate for a portion of the losses.²³ In this case, the group velocity v_g of SPPs is expected to be further slowed down.

In addition to the need for a low group velocity, a sufficiently long SPP lifetime is required to design and implement novel elements such as plasmonic waveguides or resonators.^{14,24,25} The lifetime of SPPs can be expressed as $T_{\text{SPP}}=1/(\alpha v_g)$, where α is the attenuation constant. Here, we consider a plasmonic structure covered by a dielectric grating with a constant thickness. α can be extracted from the FDTD simulated field intensity distribution,¹⁴ and v_g of SPPs can be indirectly obtained, as has been discussed before, by recording the time evolution of SPP pulse at different positions along the structure. Figure 5(a) shows the calculated magnetic field intensity ($|H_x|^2$) distributions of SPPs in a plasmonic structure in the time-position plane (along the z axis, 5 nm above the metal surface), where the central wavelength of the incident light, the grating thickness, and total length of the structure are 645 nm, 270 nm, and 100 periods, respectively. From this figure we can obtain the group velocity v_g of SPPs guided in the structure. The inset of Fig. 5(a) shows the field intensity profiles of SPPs at two positions [1.5 μm

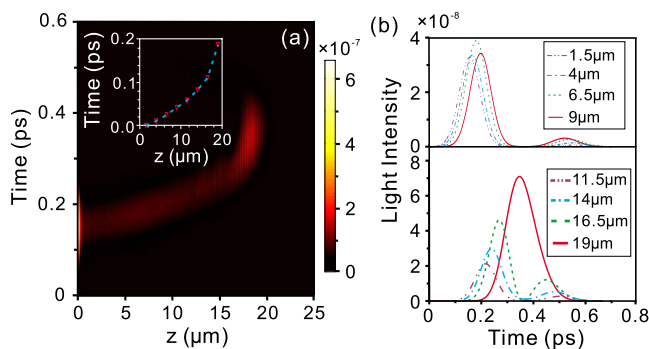


FIG. 4. (Color online) (a) Calculated gray distribution of SPP field intensity ($|H_x|^2$) in time-position plane (along the z axis, 5 nm above the metal surface). Inset: arrival time of SPP wave packets at eight spatial positions, with an equal spacing of 2.5 μm along the propagation direction. The first position is 1.5 μm away from the input port. (b) Time evolution of SPP wave packets at the above eight spatial positions of the structure. In the calculations, the incident light is a TM-polarized Gaussian pulse with a pulse width (σ) of 90 fs and 635 nm central wavelength [magnetic field is parallel to the x axis]. All the geometrical parameters are the same as that of Fig. 3(c).

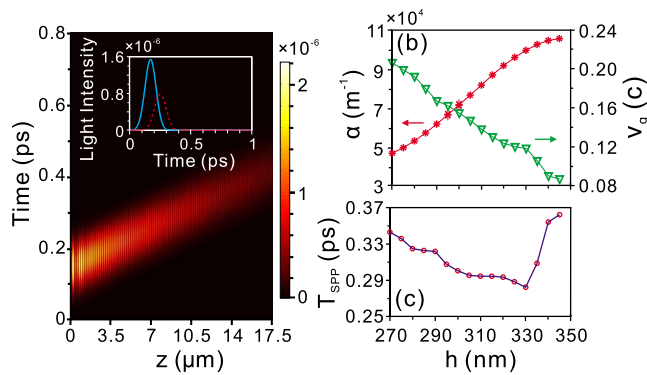


FIG. 5. (Color online) (a) Calculated magnetic field intensity distribution ($|H_x|^2$) of SPPs in the time-position plane (along the z axis, 5 nm above the metal surface) as the grating thickness and the total length of the structure are 270 nm and 100 periods, respectively. The incident pulse is the same as that used in Fig. 4 but centering at 645 nm. Inset: time evolution of the SPP intensity at two spatial positions (blue solid line: 1.5 μm and red dashed line: 6.5 μm away from the incident port). (b) and (c) Dependence of the (b) attenuation coefficient α and group velocity v_g and (c) lifetime of SPPs on grating thickness h .

(cyan solid line) and 6.5 μm (red dashed line) from the incident port, respectively]. The propagation time of SPPs from 1.5 to 6.5 μm is 81 fs, which is 4.9 times longer than that for a free space light, which means that the group velocity of the surface mode is reduced to $v_g = c/4.9$. α and v_g as functions of h are shown in Fig. 5(b). We can see that v_g is monotonically reduced with increasing h . The SPP lifetime is plotted in Fig. 5(c). In the propagation mode ($h < 330$ nm), the growth rate of α is slightly greater than the reduction rate of v_g . Thus, the SPP lifetime decreased with increased grating thicknesses. As the grating thickness is increased further, so that SPP will be localized ($h > 330$ nm), the SPP lifetime

will increase due to the greater reduction in v_g [see Fig. 5(b)]. Finally, as the grating thickness reaches the value $h = 350$ nm, the SPP lifetime reaches about 0.36 ps. This longer lifetime is on the same order of magnitude as that of plasmonic nanocrystals.²⁴ It should be pointed out that, if our proposed plasmonic structure is developed for trapped rainbow at telecommunication wavelengths, the SPP lifetime can reach several picoseconds (not shown here) due to the lower metallic absorption.

Finally, our proposed structure can also function as plasmonic color sorters²⁶ on a chip since it can separate different frequency components of the white light. For future experiment implementation, we can use chemical deposition to exactly control the thickness of the dielectric layer and employ e -beam lithography and chemical etching to etch the dielectric layer rather than the metal substrate,²⁷ which is useful for enhancing light coupling into SPPs due to the planar metal substrate-based plasmonic structures.²⁸ We can also employ nanoimprint technology to fabricate such metal-dielectric-air structures in a large scale relatively easily.²⁹ Consequently, we believe that such a structure might be “designed” freely based on the current nanofabrication technologies.

In conclusion, metal films covered by a graded dielectric grating have been demonstrated to trap true rainbows in the visible domain at different spatial positions. Our structure provides a way to slow or even trap the light signals in the nanoscale domain, offering potential applications in constructing chip-based nanoscale buffers, spectrometers, filters, data processors, and quantum optical memories.

L.C. and G.P.W. are supported by the National Basic Research Program (Grant No. 2007CB935300) and the National Natural Science Foundation of China (Grants No. 60925020, 60736041 and No. 10774116). Q.G. and F.J.B. are supported by NSF (Award No. 0901324).

*Corresponding author. Department of Physics, Wuhan University, Wuhan 430072, China; gp_wang@whu.edu.cn

¹F. Xia, L. Sekaric, and Y. Vlasov, *Nat. Photonics* **1**, 65 (2007).

²J. K. S. Poon *et al.*, *Opt. Lett.* **31**, 456 (2006).

³M. Soljacic and J. D. Joannopoulos, *Nature Mater.* **3**, 211 (2004); Y. A. Vlasov *et al.*, *Nature (London)* **438**, 65 (2005).

⁴C. W. Chou *et al.*, *Nature (London)* **438**, 828 (2005); T. Chanelliere *et al.*, *ibid.* **438**, 833 (2005).

⁵L. V. Hau *et al.*, *Nature (London)* **397**, 594 (1999); A. V. Turukhin *et al.*, *Phys. Rev. Lett.* **88**, 023602 (2001).

⁶H. Gersen *et al.*, *Phys. Rev. Lett.* **94**, 073903 (2005).

⁷Y. Okawachi *et al.*, *Phys. Rev. Lett.* **94**, 153902 (2005); Z. Zhu *et al.*, *Science* **318**, 1748 (2007).

⁸C. Liu *et al.*, *Nature (London)* **409**, 490 (2001).

⁹W. L. Barnes *et al.*, *Nature (London)* **424**, 824 (2003); E. Ozbay, *Science* **311**, 189 (2006).

¹⁰A. Karalis, *et al.*, *Phys. Rev. Lett.* **95**, 063901 (2005).

¹¹M. Sandtke and L. Kuipers, *Nat. Photonics* **1**, 573 (2007).

¹²K. L. Tsakmakidis *et al.*, *Nature (London)* **450**, 397 (2007).

¹³Q. Gan, Z. Fu *et al.*, *Phys. Rev. Lett.* **100**, 256803 (2008).

¹⁴Q. Gan *et al.*, *Phys. Rev. Lett.* **102**, 056801 (2009).

¹⁵R. J. P. Engelen *et al.*, *Phys. Rev. Lett.* **101**, 103901 (2008).

¹⁶M. I. Stockman, *Phys. Rev. Lett.* **93**, 137404 (2004).

¹⁷P. B. Johnson and R. W. Christy, *Phys. Rev. B* **6**, 4370 (1972).

¹⁸M. I. Stockman, *Nano Lett.* **6**, 2604 (2006).

¹⁹A. Yariv and P. Yeh, *Optical Waves in Crystals* (Wiley, New York, 1984).

²⁰K. S. Yee, *IEEE Trans. Antennas Propagat.* **AP-14**, 302 (1966).

²¹X. Wang and K. Kempa, *Phys. Rev. B* **71**, 233101 (2005).

²²A. Reza, *et al.*, *Nature (London)* **455**, E10 (2008).

²³J. Seidel *et al.*, *Phys. Rev. Lett.* **94**, 177401 (2005); M. A. Noginov *et al.*, *Opt. Express* **16**, 1385 (2008).

²⁴C. Ropers *et al.*, *Phys. Rev. Lett.* **94**, 113901 (2005).

²⁵P. Berini, *Opt. Express* **14**, 13030 (2006).

²⁶E. Laux *et al.*, *Nat. Photonics* **2**, 161 (2008).

²⁷R. Rao *et al.*, *Appl. Phys. Lett.* **91**, 123113 (2007).

²⁸A. V. Zayats and I. I. Smolyaninov, *J. Opt. A, Pure Appl. Opt.* **5**, S16 (2003).

²⁹S. Y. Chou *et al.*, *J. Vac. Sci. Technol. B* **14**, 4129 (1996).